THE AMERICAN SOCIETY OF MECHANICAL ENGINEERS
345 E. 47th St., New York, N.Y. 10017

97-GT-473

INFLUENCE OF TURBULENCE INTENSITY ON INTERMITTENCY MODEL IN BY-PASS TRANSITION

C.J. Hogendoorn, H.C. de Lange,
A.A. van Steenhoven† and M.E.H. van Dongen‡

Eindhoven University of Technology
Faculties of Mechanical Engineering† and Applied Physics‡
P.O. Box 513, 5600 MB Eindhoven, The Netherlands

ABSTRACT

The influence of free stream turbulence intensity on boundary layer transition was studied for a weakly compressible flow along a flat plate. The test facility consisted of a Ludwieg tube in which values of Mach number, Reynolds number and free stream turbulence could be varied over the following ranges: $0.09 < M < 0.6$, $5.10^5 < Re_u/m < 1.10^7$, $1.2\% < Tu < 9\%$. In this paper the turbulence intensity was varied up to 4.0 %. Unsteady heat flux to the flat plate was measured using cold thin film gauges. From these measurements, the intermittency was computed using an integral technique. For turbulence intensities of 1.2 %, the intermittency distribution is somewhat below the Narasimha and Johnson model, whereas a good agreement is obtained for a free stream turbulence intensity of 4.0 %. The calculated dimensionless spot production rates is proved to agree very well with existing data sets from other experiments. For a Mach number equal to 0.36 the production rates seems a bit higher when compared to the incompressible data. However, the differences are small.

NOMENCLATURE

c, c_p	specific heat, $J/kg\ K$
$F(\gamma)$	transformation function
i	electrical current, A
k	thermal conductivity, $W/m\ K$
M	Mach number
n	spot formation rate
$\hat{n}$	dimensionless spot formation rate, $n\nu^2/U^3$
P_{tot}	total dissipated power in gauges, W
Pr	Prandtl number
$\bar{q}$	averaged measured heat flux, W/m^2
R	electrical resistance, Ω
Re	Reynolds number
Re_u	unit-Reynolds number, U/ν, m^{-1}
Re_x	local Reynolds number, Ux/ν
St	Stanton number
t	time, s
T	temperature, K
Tu	turbulence intensity, $\overline{\rho u'^2}^{1/2}/\overline{\rho u}$, percent
u	velocity, m/s
x	distance from tip of the plate, m
z	coordinate perpendicular to surface, m

Greek symbols

α	temperature resistance coefficient, K^{-1}
Δz	thickness of first element, m
γ	intermittency
λ	Taylors microscale, m
λ	transition length scale, m
ν	kinematic viscosity, m^2/s
ρ	density, kg/m^3
σ	turbulent spot propagation parameter
θ	boundary layer momentum thickness, m
ξ	dimensionless scaling parameter

Presented at the International Gas Turbine & Aeroengine Congress & Exhibition
Orlando, Florida — June 2–June 5, 1997

Subscripts

0	reference situation
2nd	second nodal point from top
bot	bottom
i	initial
l	laminar
r	recovery
s	surface or start of transition
t	turbulent
ti	titanium

Abbreviations

CO	Choking Orifice
DT	Dump Tank
FP	Flat Plate
PG_i	Pressure Gauges
RTD	Resistance Temperature Device
SN	Single Normal wire probe
TG_i	Turbulence Grids
TS	Test Section

INTRODUCTION

A proper boundary layer transition model that can be used to predict the start and length of the transition region is still not available (Hirsch, 1994). Particularly in turbine blade design, it is important to predict boundary layer transition accurately because turbulent boundary layer heat transfer can be as much as 300 % greater than that for a laminar boundary layer (Consigny and Richards, 1982).

Boundary layer transition is affected by different flow parameters like pressure gradient, turbulence intensity of the main flow, heat transfer rate, surface curvature, surface roughness, etc. Different parameters have already been studied (Clark, *et al.*, 1994, Johnson and Ercan, 1996). However, the influence of higher free stream turbulence levels (characteristic for gas turbine flows) , causing so-called bypass transition is still a topic under current investigation (Mayle and Schultz, 1996). In bypass transition, turbulent spots are generated over a short distance as a result of shear layer instability, induced by free stream oscillations (Breuer and Landahl, 1990). With a description of spot growth and formation rate, an intermittency model can be constructed, which describes effectively the overall nature of boundary layer transition (Dhawan and Narasimha, 1958, Johnson and Fashifar, 1994).

In this paper we will show the change in the shape of the intermittency distribution that is brought about by an increase of free stream turbulence. The change in the intermittency will be shown on the basis of heat transfer measurements on a flat plate with sharp leading edge using cold thin film gauges (Hogendoorn *et al.*, 1996a).

The experimental set-up consists of a Ludwieg tube that allows one to vary Mach number, the unit-Reynolds number and free stream turbulence level independently over the wide range of $0.09 < M < 0.6$, $5.10^5 < Re_u/m < 1.10^7$, $1.2\% < Tu < 9\%$. In these experiments the Mach number is chosen equal to 0.18 and 0.36, while the Reynolds number is changed such that the spatial start of transition is kept constant for the different turbulence intensities.

EXPERIMENTAL SET-UP

A Ludwieg tube has been used to generate the desired flow (see Fig.1). This set-up consists of a dump

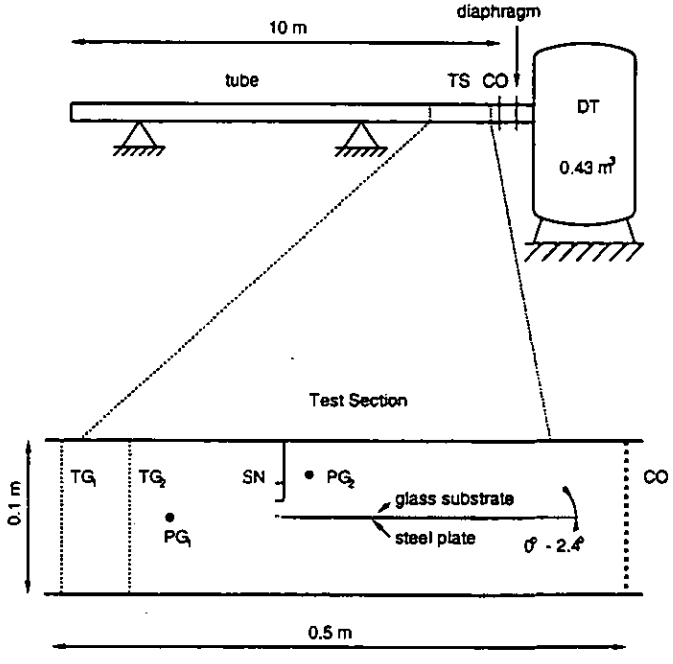

Figure 1: **The Ludwieg tube with test section.**

tank (DT) and choking orifice (CO) which is connected via the test section (TS) to a 10 meter long tube. The cross-section of the tube measures $0.1 \times 0.1m$. In between the dump tank and choking orifice, a diaphragm

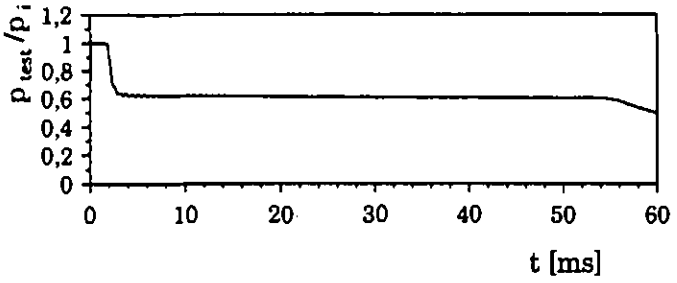

Figure 2: **Typical time trace of pressure signal (related to initial pressure) during test run, measured with PG2. The test time is about 50 ms (M=0.36, $Re_u = 6.0 \times 10^6$ $[m^{-1}]$).**

is located that separates the pressurized tube from the evacuated dump tank with a $50\mu m$ Melinex membrane. After the rupture of this diaphragm an expansion wave is generated which induces a uniform cool gas flow. This flow lasts until the expansion wave returns from the far end of the tube (about 50 ms). A typical example of pressure time trace, measured with pressure gauge PG2, is shown in Fig.2. The variation of the static pressure is less than 0.5%, which can be attributed to turbulent fluctuations in the boundary layer at the wall. Developing boundary layers at the tube wall are thin (a few millimeters) such that the flow conditions are influenced negligibly.

By using different orifice areas, the desired Mach number can be imposed. The unit-Reynolds number can be adjusted by means of the initial tube pressure. In this way the Mach and unit-Reynolds number can be chosen independently.

The averaged static pressure measured at the tube wall, deviates less than 1% from the predicted pressure according to gasdynamics. The pressure can be reproduced within 0.05% to 0.8% (depending on initial pressure level and orifice ratio).

The Mach and unit-Reynolds number are derived from recorded pressure using gasdynamical equations. Due to the difference between theoretical and measured pressure this leads to a final uncertainty in conditions of about 1% (Hogendoorn *et al.*, 1996b). Due to supersonic flow behind the orifice, disturbances can not propagate upstream from the dump tank. The upstream flow condition is constant since wave reflections (often the most disturbing phenomenon) require the same time to propagate as the expansion wave (see Fig.2). These two features give the Ludwieg tube the specific advantage to have very constant flow conditions during test time. The positive properties make the Ludwieg tube a very useful experimental set-up for the study of boundary layer transition.

Test section

The test section situated between diaphragm and tube, encloses different parts (see Fig.1). The flat plate consists of a $1.5mm$-thick stainless steel plate entirely covered by a $1.0mm$-thick glass plate (substrate for gauges). The steel plate is mounted to the side walls. The angle can be adjusted between 0° and 2.4°. With this flat plate construction the total flow blockage is minimized to about 2.5%.

An exchangeable orifice is located behind the plate. Above and in front of the plate the static pressure is recorded with a Kistler piezoelectrical pressure gauge (PG) operated with a charge amplifier (Cut-off frequency: 125 kHz). Upstream of the plate are two locations for turbulence grids (TG). Different grids have been applied with rod diameters ranging from 0.4 mm to 6 mm, with solidities in between 0.19 and 0.36. Above the leading edge of the plate, hotwire measurements have been carried out with a single normal probe (SN) in the constant temperature mode. Platinated tungsten wires of $2.5\mu m$ are applied with a length of $0.6mm$. This probe satisfies the requirements necessary to resolve the Taylor microscale, λ (Bruun,1995). The overheat ratio has been set at 1.6.

The turbulence intensity has been measured at 10 and $20mm$ above the plate. The turbulence grids have been chosen such that turbulence intensities between 1.2% and 9% can be created. The free stream turbulence level is very constant during the experiment and reproduces always within 4%.

Cold thin film gauges

Unsteady heat flux measurements were acquired using thin titanium film gauges. These sensors are used as resistance temperature devices (RTD's) to measure the surface temperature without influencing the heat transfer process. The titanium sensors are evaporated onto a 1.0 mm thick B270-glass substrate with accurately known substrate properties. 33 gauges were used

in a special two-dimensional configuration (see Fig.3) to measure both the individual spot properties and average intermittency over the transition region. Two

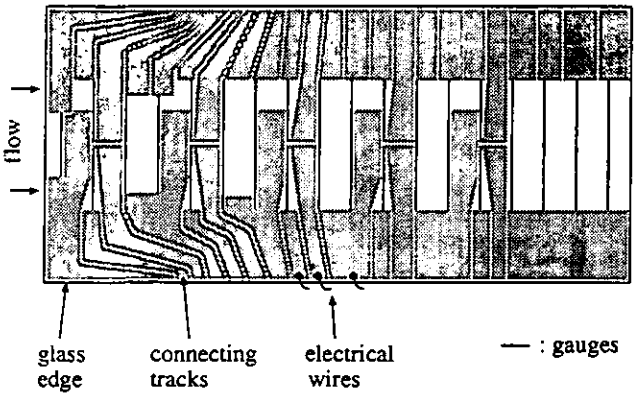

Figure 3: **Top view sketch of the sensor lay out on glass substrate. The solid lines represent the locations of the sensors (drawn with exaggerated thickness).**

different sensor dimensions are used: 13 long gauges of 40 mm [1] $\times$ 50 μm (length $\times$ width) and 5 rows of 4 small gauges of 9.5 mm $\times$10 μm. The mutual sensor distance in flow direction is 10 mm. The sensor thickness is about 70 nm which yields a response frequency of the film upto 100 MHz (Diller,1993). The effective frequency of total heat flux measuring system is limited by the operational amplifier (about 80 kHz). The sensors were designed according to an optimization strategy which balances the effect of sensor heating due to dissipation (low current) and the required accuracy (high current).

The sensor resistance depends on the temperature according to the relation

$$R_{sensor} = R_0 [1 + \alpha_0 (T_{sensor} - T_0)] \qquad (1)$$

Here R_0 is the initial sensor resistance, T_0 the initial sensor temperature and α_0 the resistance temperature coefficient at reference condition. After gauging, the value for the resistance temperature coefficient of titanium, α_{ti}, is found to be equal to $1.77 \times 10^{-3}\ K^{-1}$ ($\pm 5\%$). The current per sensor, i, is chosen between 1 to 2 mA, with its specific value being dependent on its resistance. In this paper 16 gauges at individual distance of 10 mm are employed for intermittency measurements.

[1] one gauge of 20 mm and two gauges of 30 mm

Data acquisition

In order to measure only the fluctuations in heat transfer, measurements were acquired with a 0.25 kHz high-pass filter. This signal is amplified with a one-step operational LF356 differential amplifier with an amplification rate of 100.0. The data is read using a 12-bit AT-MIO-16E-1 I/O board mounted in a 486DX-PC. The total sample frequency available was 1.2 MHz. For 16 channels, this results in a sample frequency of about 60 kHz. The board was controlled by the software package Labview. An arbitrary sensor signal is used to trigger the measurement system.

As a result of circuit noise and noise generated by machines in the surroundings, a certain noise level is present on the signal. To decrease this noise level, all wires were shielded and potential noise sources in the surroundings were checked individually on their effect. Furthermore, groundloops were avoided and the Ludwieg tube was grounded. The final heat flux rms-value due to noise is 70 W/m^2.

Flux reconstruction

The unsteady heat flux at the surface can be reconstructed by solving the unsteady 1-D conduction equation

$$\rho c \frac{\partial T}{\partial t} = \frac{\partial}{\partial z}\left(k \frac{\partial T}{\partial z}\right) \qquad (2)$$

for the glass substrate[2].

The required glass-substrate properties are known (k=0.92 W/mK, ρ=2550 kg/m^3, c= 860 J/kgK). Due to the short experimental time, the thermal front does not reach the bottom side of the glass substrate. Therefore, the temperature at the bottom, $T_{bot}(t)$, is constant. The temperature at the top, $T_{top}(t)$, is measured with the sensor. Prescribing these known temperatures and the substrate properties, the unsteady temperature profile in the glass substrate can be computed numerically. The unsteady flux at the surface, $q_s(t)$, is then reconstructed by

$$q_s(t) = k \frac{T_{top}(t) - T_{2nd}(t)}{\Delta z} \qquad (3)$$

where $T_{2nd}(t)$ is the temperature in the second nodal point and Δz is the thickness of the first computational

[2] The film thickness is negligibly small

element. A typical example of instanteneous heat flux measured by a 9.5 mm-gauge is shown in Fig.4. Because the sensor length is comparable with the turbulent spot size, the passing spots are clearly visible by increasing heat flux rate.

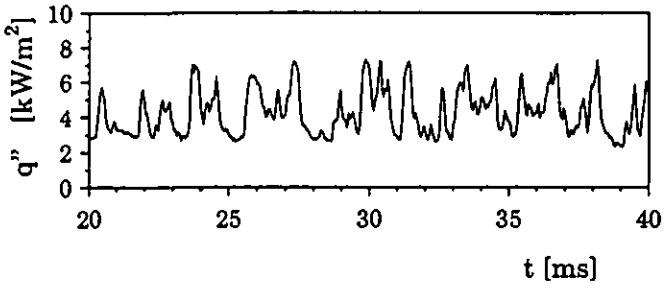

Figure 4: **Typical heat flux measured at a flat plate in the Ludwieg tube at $x = 103mm$ from leading edge. The individual turbulent spots are clearly recognizable ($M = 0.36$, $Re_u = 4.9 \times 10^6$, Tu=1.7%).**

DATA PROCESSING

Dissipation in the 33 gauges ($P_{tot} \approx 1.1\ W$) causes the flat plate temperature to increase slightly. This temperature rise stabilizes at constant uniform temperature of 2 K after about 15 minutes. Since the temperature difference between plate and gas is only about 30 K, a small sensor temperature rise of $2K$ will produce a deviation in heat flux of about 6%.
Another deviation (of about 5%) is caused by differences in temperature resistance coefficients, α_0, of different sensors. This coefficient has not been determined for each sensor separately.

To correct for these errors, an in-situ calibration has been applied to correct the data to get optimum accuracy. This has been done using a flow of low turbulence intensity and low Reynolds number that gives a complete laminar boundary layer along the plate. For this calibration the instantaneous heat flux has been checked and found to be completely laminar (no turbulent spots were observed). The measured heat flux is then compared to the theoretical curve for heat transfer in a laminar boundary layer as given by the Blasius solution (Schlichting, 1979)

$$q_l(x) = 0.332 \frac{k(T_{wall} - T_r)}{x} Re_x^{1/2} Pr^{1/3} \qquad (4)$$

where k is the thermal conductivity, $T_{wall} - T_r$, the difference between wall and recovery temperature, Re_x is the Reynolds number based on the distance, x, from the leading edge of the plate, and Pr is the Prandtl number.

The nature of the deviation due to dissipation will cause the experimental heat transfer to be somewhat higher than the theoretical curve. This is confirmed by the comparison shown in Fig.5. It was verified that the deviations are not caused by stochastic errors. To correct the experimental fluxes to the theoretical values, the signal is multiplied with an individual calibration factor for each sensor separately, based on the data of Fig.5. In the following experiments these same factors are used to correct the measured heat fluxes. The uncertainty of the measured heat flux is found to be at maximum 1.5% after calibration.

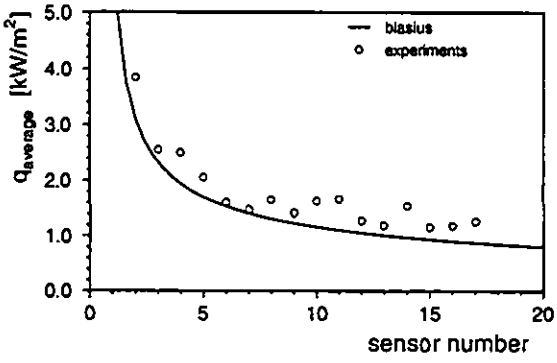

Figure 5: **Uncorrected data compared with the theoretical heat transfer rate. $Re_u/m = 2.51.10^6$, $M = 0.36$, $T_{wall} - T_{recovery} = 32.5K$, $Tu = 1.2\%$ in air.**

For the determination of the intermittency the averaged heat flux has been used. Because the turbulent spots do not cover the complete sensor, the instanteneous data can not easily be used to determine the intermittency using indicator functions. Therefore, the averaged heat flux has been applied according to Dhawan and Narasimha (1958).

The average surface heat flux, $\overline{q_s(x)}$, is calculated at each gauge location from:

$$\overline{q_s(x)} = \frac{1}{t_2 - t_1} \int_{t_1}^{t_2} q_s(x,t) dt \qquad (5)$$

with t_1 and t_2 the beginning and end of the test period, respectively.

From this the intermittency, γ, is computed (Dhawan and Narasimha, 1958):

$$\gamma(x) = \frac{\overline{q_s(x)} - q_l(x)}{q_t(x) - q_l(x)} \quad (6)$$

Hereby, the theoretical values for both the laminar, q_l, (according to Eq.4) and turbulent heat flux, $q_t(x)$, are applied, using the empirical curve for a fully developed turbulent boundary layer given by (Schlichting, 1979):

$$q_t(x) = C(Tu)0.0288\frac{k(T_{wall} - T_r)}{x}Re_x^{4/5}Pr^{1/3} \quad (7)$$

Here $C(Tu) \approx 1 + 0.05Tu$ which account for the contribution of the free stream turbulence level (Blair,-1983, Simonich and Bradshaw, 1978). However, due to scatter in the literature, the empirical relation has an uncertainty of a few percent. To eliminate this small uncertainty the empirical turbulent relation has been adjusted to the turbulent level obtained in the experiment.

An example is shown in Fig.6, with the laminar and turbulent relation in terms of the Stanton number, $St = \frac{q}{(T_{wall}-T_r)\rho c_p u}$. The ratio according to Eq. 6 at each location provides the intermittency, $\gamma(x)$.

The intermittency distribution for one single run, reproduce within 2% for the whole range of flow conditions. This means that a single run for each combination of flow conditions is sufficient. However, to improve the reliability, each experiment was performed two times.

RESULTS

As discussed before, turbulence intensities of up to 9% can be generated in the facility. However, it is observed that the tangent of the plate angle must be on the order of the turbulence intensity to have a proper laminar boundary layer downstream of the leading edge. This not well-documented effect can be interpreted physically as follows. Because of turbulent fluctuations, the free stream 'velocity vector' will vary with an angle equal to about the tangent of the free stream turbulence. Turbulent fluctuations producing an angle of incidence larger than the plate angle will cause boundary layer separation at the sharp leading edge of the plate. The current construction allows a maximum angle of about 2.4° which corresponds to a maximum free stream turbulence of about 4%.

Next, it is investigated whether the transition process is angle-dependent for angles above the 'critical' value. This has been done for a flow with a free stream turbulence intensity of 2.2%. The 'critical' plate angle is found to be 0.93° ($tan0.93°$=0.016). The plate angle has been stepwise increased to 2.3°. It turned out that no differences in the boundary layer transition behaviour are found for the angles in the range of 1° to 2.3°. From this result it may be concluded that these small angles does not induce a pressure gradient.

The experiments were performed for plate inclinations slightly above the critical angles. Boundary layer transition has been studied at a constant Mach number for different free stream turbulence intensities. In order to have sufficient gauges in the transition region the unit-Reynolds number was varied, so that the length of transition occured over about ten sensors. Turbulence intensity was varied in the range from 1.2% to 4.0%. In Fig.6 measured values of heat flux along the plate, expressed in the Stanton number, are presented as a function of Reynolds number. The straight course

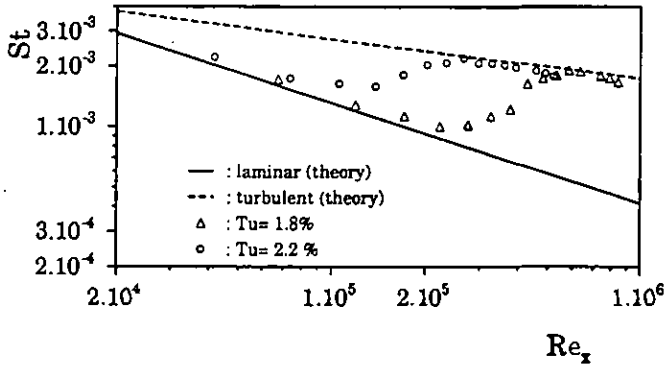

Figure 6: **Stanton numbers versus Re_x for different free stream turbulence intensities.** $M = 0.36$, $T_{gas} - T_{recovery} = 32.5K$.

of the boundary layers at the very beginning indicate clearly the laminar start. The level of the first gauges corresponds to the Blasius solution (Eq.(4)). At the end, the boundary layer is fully turbulent.

The transition Reynolds number has been determined by a least square fit through the intermittency distribution using the transformation $F(\gamma) = (-ln(1-\gamma))^{1/2}$ according to the Narasimha model (Gostelow

and Blunden, 1989). The transition Reynolds number, Re_s, is defined at the number where the intermittency (in the fit) is zero. A typical example is shown in Fig.7. The transition Reynolds number can be used to com-

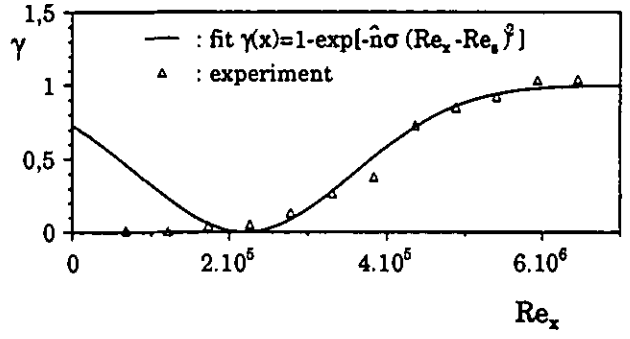

Figure 7: **Least square fit through the intermittency obtained from the experiment (M=0.36, $Re_u = 5.25 \times 10^6$ $[m^{-1}]$, Tu=1.8%).**

pute the Reynolds number based on the boundary layer momentum thickness at the start of transition, $Re_{\theta,s}$. According to the Blasius solution this number is given by $Re_{\theta,s} = 0.664\sqrt{Re_s}$ (Schlichting, 1979).

Figure 8 shows this Reynolds number versus the free stream turbulence intensity for M=0.18 and 0.36, together with experimental results obtained from the literature. It is shown that the present results cor-

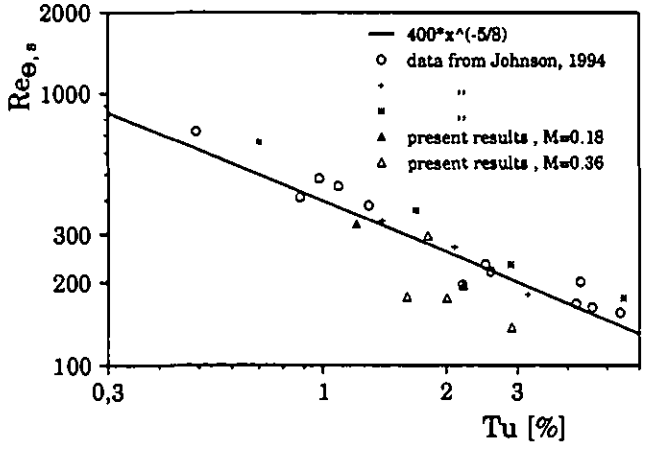

Figure 8: **Reynolds number based on the boundary layer momentum thickness at the start of transition, $Re_{\theta,s}$, versus free stream turbulence intensity.**

respond with other results (Johnson, 1994). Increasing free stream turbulence causes decreasing Reynolds number based on momentum thickness at transition start. Some experiments show a somewhat lower transition Reynolds number.

Another comparison concerns the intermittency as a function of ξ, the dimensionless scaling parameter. ξ is defined as $(x - x_s)/\lambda$, with $x_s = Re_s/Re_u$, the start of transition and $\lambda = (x_{\gamma=0.75} - x_{\gamma=0.25})$. A typical result is shown in Fig.'s 9 and 10 for flow with different free stream turbulence levels. This intermittency is compared with the Narasimha (Dhawan and Narasimha, 1979) and Johnson (Johnson and Fashifar, 1994) model given respectively by

$$\gamma = 1 - exp(-0.412\xi^2) \tag{8}$$

and

$$\gamma = 1 - exp(-0.0941\xi^3) \tag{9}$$

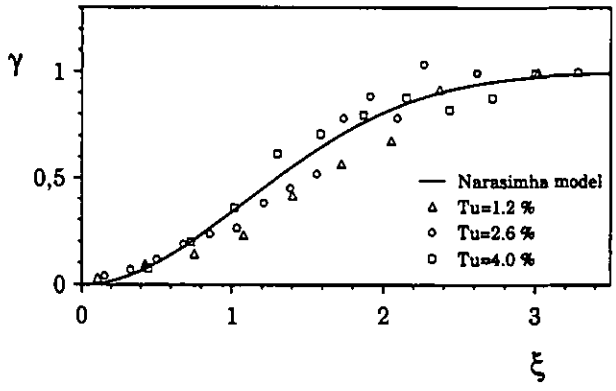

Figure 9: **Intermittency comparison with the Narasimha model for experiments with free stream turbulence levels of 1.2, 2.6 and 4.0 % (M=0.18).**

It is observed that the intermittency distribution according to the Johnson model is a bit more close to the model prediction than that for the Narasimha model. However, the differences are small. Furthermore, it can be seen that the free stream turbulence level has a weak influence on the intermittency distribution. The intermittency for the turbulence level of 1.2% has a distribution below the Narasimha and Johnson model, whereas the intermittency for the experiment with Tu=4.0% matches to both models very well. The experiment with 2.6% is located in between.

The transition lengths for the different experiments

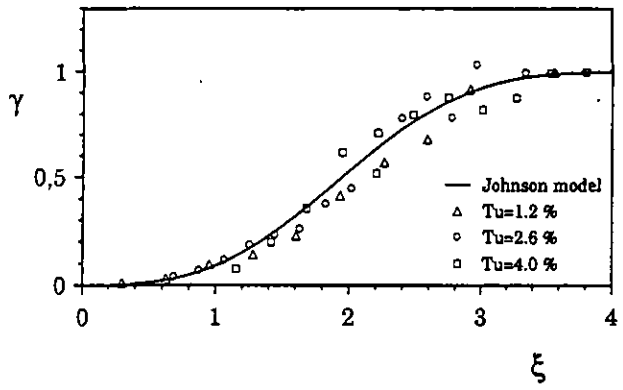

Figure 10: **Intermittency comparison with the Johnson model for experiments with free stream turbulence levels of 1.2, 2.6 and 4.0 % (M=0.18).**

are compared with the intermittency distribution by Dhawan and Narasimha (1958) rewritten as (Mayle, 1991)

$$\gamma = 1 - exp\left[-\hat{n}\sigma(Re_x - Re_{tr})^2\right] \qquad (10)$$

where $\hat{n} = n\nu^2/U^3$ is the dimensionless spot production parameter. The fits for different experiments are shown in Fig.11 given by the solid lines. The dashed lines are two experimental curves from Mayle (1991) for free stream turbulence intensities of 1 % and 10 %. Present experimental curves are clearly within this

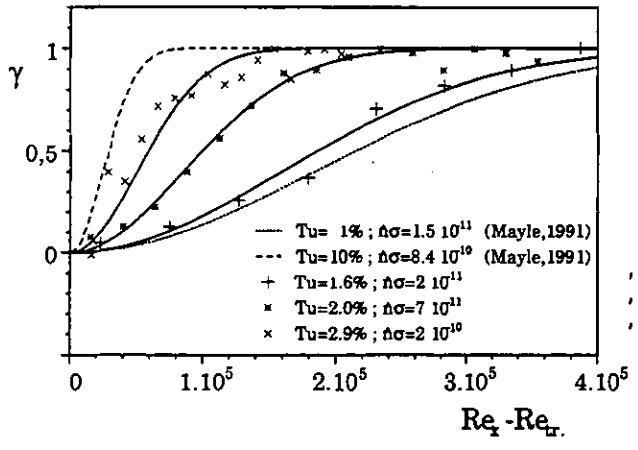

Figure 11: **Intermittency for different turbulence intensities in comparison with the dimensionless spot formation rate, $\hat{n}\sigma$. The solid lines are the best fit functions through the data (M=0.36).**

range. From these fits the dimensionless spot production rate versus the free stream turbulence intensities are obtained. These are compared with experimental data given by Mayle (1991) in Fig.12. Mayle proposed

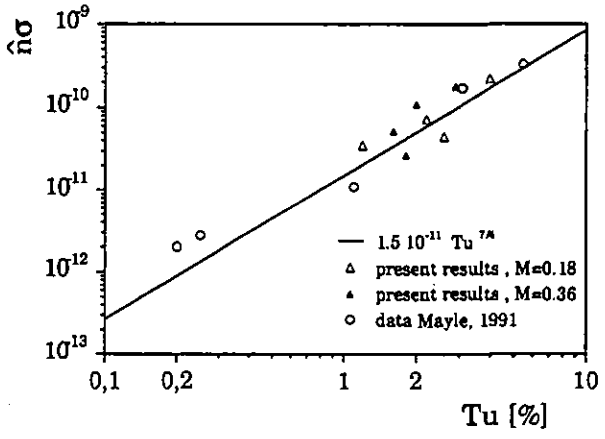

Figure 12: **Spot production rate as a function of free stream turbulence level in comparison to other data.**

the experimental fit given by

$$\hat{n}\sigma = 1.5 \times 10^{-11} Tu^{7/4} \qquad (11)$$

The present results correspond very well with the fit. For a Mach number equal to 0.36 the spot production rate seems to be a slightly higher. However, the differences are not significant compared to results for M=0.18 and the incompressible data of Mayle.

CONCLUDING REMARKS

Boundary layer transition has been studied using cold thin film gauges measuring the heat flux to a flat plate with sharp leading edge. A Ludwieg tube has been used as experimental set-up which can generate flows with well known conditions over a wide range. Experiments can be reproduced with very high accuracy. The available free stream turbulence intensities range from 1.2 % up to 9 %. However, it is shown that for a flat plate with sharp leading edge the plate angle must be about the inverse tangent of the turbulence intensity to prevent boundary layer separation at the very beginning. Because the plate angle was adjustable to the limit of 2.4°, the turbulence intensity has been varied to 4.0 %. The Mach number which can be adjusted has been chosen to be 0.18 and 0.36, while the unit-Reynolds number has been adjusted to have transition over the whole sensor plate.

The start of the transition Reynolds number, $Re_{\theta,s}$,

as function of free stream turbulence intensity has been found to correspond very well with results from the literature. The intermittency is computed on the basis of time averaged heat flux according to the definition of Narasimha (Dhawan and Narasimha, 1958). It is found that the intermittency distribution according to the Johnson model shows a slightly better correspondence to the model, when compared to the Narasimha model. However, the differences are small. The intermittency for the turbulence level of 1.2% has a distribution below the Narasimha and Johnson model, whereas the intermittency for the experiment with 4.0% matches both models very well. The experiment with 2.6% is situated in between. A reason for this turbulence level dependency as compared to previous measurements (e.g.(Gostelow *et al.*, 1994)) may be found in the fact that the intermittency in our experiments is computed on the basis of the integral heat flux.

The dimensionless spot production rates obtained correspond very well with wind tunnel experiments. For experiments with Mach number equal to 0.36, the spot production rates seem to be a slightly higher in comparison to the incompressible data. However, these differences are small and more experiments at higher Mach numbers are needed to make final conclusions possible.

ACKNOWLEDGEMENTS

The authors are grateful to Ir. R. Schook, R. den Biggelaar and M. Risseeuw for their assistance in the experiments performed.

REFERENCES

Blair, M.F., 1983, "Influence of free-stream turbulence on turbulent boundary layer heat transfer and mean profile development, Part I - experimental data," *ASME Journal of Heat Transfer*, vol. 105, pp.33-40.

Breuer, K.S. and Landahl, M.T., 1990, "The Evolution of a Localized Disturbance in a Laminar Boundary Layer. Part 2. Strong Disturbances," *Journal of Fluid Mechanics*, vol. 220, pp.595-621.

Bruun, H.H., 1995, "Hot-Wire Anemometry (Principles and Signal Analyses)," *Oxford University Press.*

Clark, J.P., Jones, T.V. and LaGraff, J.E., 1994, "On the Propagation of Naturally-Occurring Turbulent Spots," *Journal of Engineering Mathematics*, vol. 28, pp.1-19.

Consigny, H. and Richards, B.E., 1982, "Short Duration Measurements of Heat Transfer Rate to a Gas Turbine Rotor Blade," *Journal of Engineering Power*, vol. 104, pp.542-551.

Dhawan, S. and Narasimha, R., 1958, "Some Properties of Boundary Layer Flow during the Transition from Laminar to Turbulent Motion," *Journal of Fluid Mechanics*, vol. 3, pp.418-436.

Diller, T.E., 1993, "Advances in Heat Flux Measurements," *Advances in Heat Transfer, ed. J.P. Hartnett etal. Academic Press, Inc.*, vol. 23.

Gostelow, J.P. and Blunden, A.R., 1989, "Investigations of boundary layer transition in adverse pressure gradient," *Journal of Turbomachinery*, vol. 111, pp.366-375.

Gostelow, J.P., Blunden, A.R. and Walker, G.J., 1994, "Effects of Free-Stream Turbulence and Adverse Pressure Gradients on Boundary Layer Transition," *Journal of Turbomachinery*, vol. 116, pp.393-404.

Hirsch, Ch., 1994, "CFD Methodology and Validation for Turbomachinery Flows," *Turbomachinery Design Using CFD*, AGARD-LS-195, pp.4.1-4.44.

Hogendoorn, C.J., de Lange, H.C. and van Steenhoven, A.A., 1996a, "Heat Transfer Measurements in Transitional Boundary Layers," *Proceedings of 2nd European Thermal Sciences and 14th UIT National Heat Transfer Conference*, Edizioni ETS, pp.593-600.

Hogendoorn, C.J., de Lange, H.C., van Steenhoven, A.A., and van Dongen, M.E.H., 1996b, "The adequacy of Shock and Ludwieg Tube for Turbulent Spot Research," *Submitted.*

Johnson, M.W., 1994, "A Bypass Transition Model for Boundary Layers," *Journal of Turbomachinery*, vol. 116, pp.759-764.

Johnson, M.W. and Ercan, A.H., 1996, "A Boundary Layer Transition Model," *International Gas Turbine and Aeroengine Congress and Exhibition*, 96-GT-444.

Johnson, M.W. and Fashifar, A., 1994, "Statistical Properties of Turbulent Bursts in Transitional Boundary Layers," *International Journal of Heat and Fluid Flow*, vol. 15, pp.283-290.

Mayle, R.E., 1991, "The Role of Laminar-Turbulent Transition in Gas Turbine Engines," *Journal of Turbomachinery*, vol. 113, pp.509-537.

Mayle, R.E. and Schultz, A., 1996, "The Path to Predicting Bypass Transition," *International Gas Turbine and Aeroengine Congress and Exhibition*, 96-GT-199.

Schlichting, H., 1979, *"Boundary-Layer Theory"*, McGraw-Hill Book Company, seventh edition.

Seifert, A., Zilberman, M. and Wygnanski, I., 1994, "On the Simultaneous Measurement of Two Velocity Components in the Turbulent Spot," *Journal of Engineering Mathematics*, vol. 28, pp.43-54.

Simonich, J.C. and Bradshaw, P., 1978, "Effect of free-stream turbulence on heat transfer through a turbulent boundary layer," *ASME Journal of Heat Transfer*, vol. 100, pp.672-677.